www.ietdl.org

Published in IET Power Electronics
Received on 1st December 2011
Revised on 18th March 2013
Accepted on 11th May 2013
doi: 10.1049/iet-pel.2012.0570

ISSN 1755-4535

Reciprocal effects of the distorted wind turbine source and the shunt active power filter: full compensation of unbalance and harmonics under 'capacitive non-linear load' condition

Bijan Rahmani, Mohammad Tavakoli Bina

Faculty of Electrical Engineering, K. N. Toosi University of Technology, Seid Khandan, P.O. Box 16315-1355, Tehran 16314, Iran
E-mail: Bijan_x1461@yahoo.com

Abstract: Available compensating algorithms for shunt active power filters (SAPFs) and unified power quality conditioner perform somehow improperly in practice under certain circumstances. Typical examples could be any distorted 'non-linear loads' showing low impedances at certain frequencies; also, there are technological limitations for the SAPF in modulating switching frequencies, including microcontroller processing speed, the employed control and modulation techniques, delays and so on. This study proposes an advanced universal power quality conditioning system (AUPQS) to fine tune the available solutions for generating purely sinusoidal wind turbine-end currents under both distorted-unbalanced load-terminal voltages and non-linear load conditions (capacitive loads leave much worse consequences than those of the inductive). It is shown that both series and SAPF are capable of full compensation of microgrid by the SAPF using the advanced generalised theory of instantaneous power. Meanwhile, the resultant source currents could be somehow non-sinusoidal. However, the proposed AUPQS will be able to fully eliminate the consequence of voltage asymmetry and unbalanced waveforms on the SAPF, generated because of the wind turbine operation by performing certain corrections on these solutions. Moreover, an independent single-phase rectifier is proposed at the load-end to regulate DC-link voltage. Effectiveness of the proposed AUPQS is confirmed by Simulink simulations.

1 Nomenclature

SAPF	shunt active power filter
AUPQS	advanced universal power quality conditioning system
A-GTIP	advanced generalised theory of instantaneous power
AR	active rectifier
SF	series filter
GTIP	generalised theory of instantaneous power definition
V_{S}	source voltages
V_{L}	load-terminal voltages
V_{VR}	voltage type load
V_{SF}	SF voltages
V_{L1}^{+}	fundamental sequence of positive component of load-terminal voltages
V_{S}^{+}	positive component of source voltages
V_{S}^{-}	negative component of source voltages
V_{S}^{0}	zero component of source voltages
$V_{\mathrm{S}1}{}^{+}$	fundamental sequence of positive component of source voltages
$V_{\mathrm{reference}}$	SF reference voltage
$V_{\mathrm{L\text{-}AUPQS}}$	load-terminal voltages compensated by the AUPQS
$V_{\mathrm{L\text{-}UPQC}}$	load-terminal voltages compensated by the UPQC
I_{L}	load-end currents
I_{S}	source-end currents
i_{S}^{+}	positive component of source-end currents
i_{S}^{-}	negative component of source-end currents
i_{S}^{0}	zero component of source-end currents
I_{C}	SAPF reference currents
I_{SAPF}	SAPF injected currents
$I_{\mathrm{S\text{-}AUPQS}}$	source-end currents compensated by the AUPQS
$I_{\mathrm{S\text{-}UPQC}}$	source-end currents compensated by the UPQC
$\mathrm{I}_{\mathrm{disturbance}}$	source-end current harmonics
$I_{\mathrm{reference}}$	SAPF reference currents
K	impedance gain of the SF
$Z_{\mathrm{S}}(\mathrm{j}\omega)$	series impedance of the system supply
$Z_{\mathrm{L}}(\mathrm{j}\omega)$	series impedance of load

2 Introduction

Rapid growth of non-linear loads leads to lots of power quality problems such as harmonics, unbalance operation and excessive source-end neutral current in three-phase supplying networks. These power quality problems cause many adverse effects like errors in measuring instruments, accentuation of harmonics, false operation of circuit breakers and relays, reduction in transmission system efficiency, malfunction in electronic equipment and overheating of transformers [1]. A common compensation algorithm is the optimal solution (OS) [2, 3]. The OS is simple to implement, applicable only to three-wire balanced systems. Further, the generalised theory of instantaneous power (GTIP) definitions was proposed [4]. It is shown in [5, 6] that the GTIP can be derived from the OS. Although the compensation algorithm based on the GTIP has an acceptable performance in three-phase four-wire balanced systems, distorted source-end zero sequence current is unavoidable under non-ideal waveforms [6]. Other prominent proposed power theories are Fryze, Buchholz and Depenbrock (FBD) [7], current's physical component [8] (in the frequency domain interprets and describes power phenomena in three-phase three-wire systems), conservative power theory [9] and the p–q–r theory [10–12] (defined in α–β–0 reference frame). The control algorithms based on these power theories provide accurate references for active power filters.

However, these theories result in unsatisfactory outcomes when the plant includes wind turbine systems. This happens because of the 3rd, 5th, 7th and 11th harmonics produced by the wind turbine [13, 14]. Either a compensating algorithm or a proper physical structure should be applied according to the desired objectives. In [15], two solutions were proposed to improve the shunt active power filter (SAPF) performance when the source voltages are distorted (e.g. unsymmetrical or unbalanced voltage waveforms produced because of the wind turbine operation). The first solution suggests a compensation algorithm based on the advanced GTIP (A-GTIP) theory. The second solution proposes a series filter (SF) to compensate the point of common connection voltage [15, 16]. Nonetheless, the SAPF introduces unacceptable performance even under these solutions. This could be worsening in the presence of non-linear capacitive loads [17]. Big capacitive loads in power systems include power factor correction capacitors and filters. The majority of effective capacitance is only added to correct inductive reactance for power factor. Also, the non-linear switching and electronic loads have lots of internal capacitors. Meanwhile, the rejection of real component of the load or tripping other generators feeding the same capacitive load in supply networks would lead to a possible capacitive load condition. Also, the low impedance of capacitive loads at a certain harmonic can be seen dominantly as the dominant load at that harmonic.

This paper intends to improve and/or fine tune the aforementioned solutions for a satisfactory cancellation of the wind turbine-end current harmonics by suggesting both required power circuit and a fine tuning control loop. An advanced universal power quality conditioning system (AUPQS) is proposed which leads to purely sinusoidal source-end currents under both distorted-unbalanced load-terminal voltages and non-linear load conditions. Moreover, the isolated DC-link voltage is regulated by using a single-phase converter connected across the load-terminal. Thus, unlike the earlier three-phase converter proposition at the 'source-end' [17], the new suggestion will be able to regulate the DC-link voltage without any further distortion. In fact, the generated distortions by the AR are compensated via the shunt filter of the proposed AUPQS. This is also applied to a simulated wind farm in order to attenuate frequency variations provided because of the torsional torque vibrations [18–20] of a wind farm. This paper introduces initially the mathematical analysis that discusses elimination of the non-ideal voltage waveforms because of the wind turbine operation; in particular, under distorted non-linear capacitive/inductive load conditions. Then, essential corrections are applied to the proposed solutions in [15], and it will be shown that a combination of these improved solutions is necessary for immunising the wind energy source from the load harmonics. Further, an AUPQS is suggested for three-phase four-wire systems, where simulations verify effective performance of the AUPQS in line with the desirable outcomes.

3 Practical issues and the suggested improvements

There are two solutions for improving accuracy of the SAPF when the voltages of a wind plant are non-ideal. These solutions are presented here. Then, their validities will be analysed under non-linear loads.

3.1 Compensating with the A-GTIP theory

SAPF is used to eliminate load-terminal current harmonics, leading to purely sinusoidal source-end currents [21, 22]. The GTIP definition is usually used for reference signal determination in the compensation schemes for shunt active filters. Let us suppose that wind turbine voltage (V_S(t)) involves all sequences$\left(V_S(t) = v_S^+(t) + v_S^-(t) + v_S^0(t)\right)$, where $v_S^+(t)$, $v_S^-(t)$ and $v_S^0(t)$ are positive, negative and zero sequence components of $V_S(t)$, respectively. On the other hand, the absence of series active filter or series impedances results in source-end fixed voltages, that is, the load-terminal voltages. Therefore the source-end currents (I_S) and the reference currents of the SAPF (I_C), using the OS [2, 3] can be rewritten as

$$\begin{cases} I_S(t) = i_S^+(t) + i_S^-(t) + i_S^0(t) = \lambda\, v_S^+(t) + \lambda\, v_S^-(t) + \lambda\, v_S^0(t) \\ \lambda = \dfrac{\bar{P}(t)}{V_S(t)\, V_S(t)} \\ I_C(t) = I_S(t) - \dfrac{\bar{P}(t)}{V_S(t)\, V_S(t)} V_S(t) \end{cases} \tag{1}$$

Since the non-sinusoidal term V_S (t) in (1) acts as a source of distortion, the SAPF compensation algorithm will inject a distorted current. Therefore the compensation algorithm derived from the GTIP under both asymmetric and distorted three-phase load-terminal voltages provides unacceptable outcomes. The A-GTIP theory takes (1) one step forward in order to overcome the stated issue by replacing $V_S(t)$ with $V_S^+(t)$ in (1) as follows

$$I_S(t) = \frac{\overline{P}^+(t)}{V_S^+(t)\, V_S^+(t)} V_S^+(t) \tag{2}$$

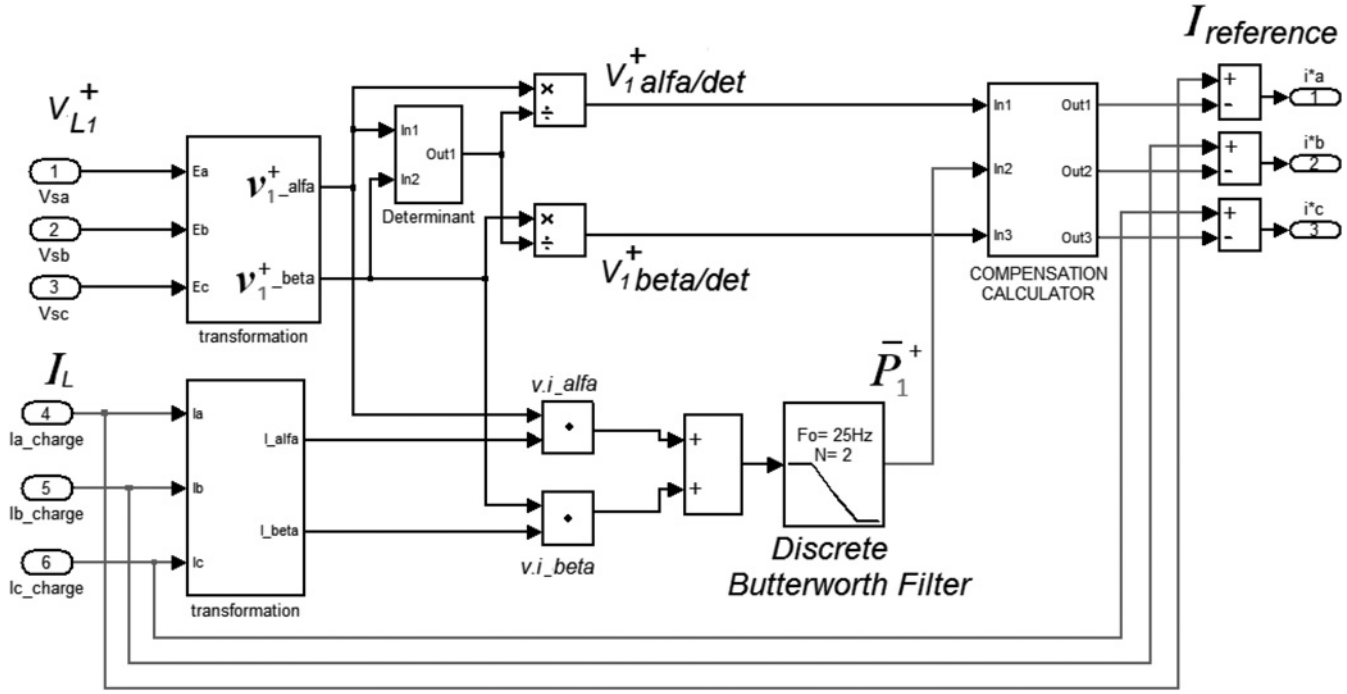

Fig. 1 *A-GTIP algorithm stated in [6]*

As long as $V_S^+(t)$ is the fundamental component of $V_S(t)$, the source-end currents remain purely sinusoidal. Otherwise, the non-sinusoidal $V_S^+(t)$ would generate distortions [6]; therefore the SAPF compensation algorithm will inject a distorted current. The block diagram of the A-GTIP is shown in Fig. 1.

The proposed solution in [15] performs unexpectedly when a non-linear load shows a very low impedance in some frequency components [see $Z_L(j\omega_h)$ in Fig. 2]. The injected current by the SAPF (I_{SAPF}) cannot perfectly compensate the load harmonics [$G(j\omega_h) < 1$ in Fig. 2] because of the stated low impedance together with the aforementioned technical limitations. Therefore the source-end currents would be non-sinusoidal. Hence, arranging a KCL at the load terminal as well as a KVL within the available loop will lead to

$$\begin{cases} I_S = (1 - G(j\omega))I_L \\ V_S = Z_S I_S + Z_L\big(I_S + G(j\omega)I_L\big) + V_{VR} \end{cases} \tag{3}$$

where $G(j\omega)$ is the transfer function relating I_L to I_{SAPF}. Both the load current $I_L(t)$ and the source-end current $I_S(t)$ can be obtained for a given ω as follows

$$\begin{cases} I_L(j\omega) = \dfrac{V_S(j\omega) - V_{VR}(j\omega)}{Z_L(j\omega) + (1 - G(j\omega))Z_S(j\omega)} \\ I_S(j\omega) = \dfrac{V_S(j\omega) - V_{VR}(j\omega)}{(1 - G(j\omega))Z_S(j\omega) + Z_L(j\omega)}(1 - G(j\omega)) \end{cases} \tag{4}$$

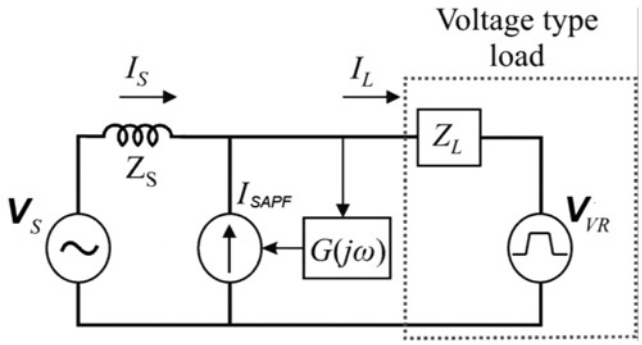

Fig. 2 *Compensation issue related to shunt active filter under voltage type capacitive loads*

In practice, at a certain harmonic (e.g. $\omega = \omega_h$) the relationship $(1 - G(j\omega))|_{\omega=\omega_h}$ is non-zero, resulting in non-zero source-end current according to (4). This implies that the given harmonic ($\omega = \omega_h$) cannot be fully compensated by the SAPF. Also, it should be emphasised that non-zero source current occurs because of the technical limitations for all practical load conditions under certain harmonics. This drawback is described by the simulated active filters in Fig. 14*b*. Additionally, even if $(1 - G(j\omega))|_{\omega=\omega_h}$ is zero, then a very low $Z_L(j\omega)$ results in a non-zero source-end current; once again imperfect compensating operation of the SAPF. For example, the stated situation can happen when single-phase and/or three-phase diode rectifiers terminated by capacitances are connected across the load-terminal. Under these typical circumstances, the AC-side of the load-terminal sees effectively a very low non-zero $Z_L(j\omega)$ in most harmonics. Therefore active filters cannot produce satisfactory outcomes as can be seen in simulations shown in Fig. 14*b*, where the THD of the $I_{S\text{-}AUPQS}$ is 3.36% for $K = 0$ under a capacitive non-linear load. One solution could be inclusion of an SF as follows.

3.2 Series filter

An active SF is used as a solution to remove the effects of wind turbine asymmetric and distorted voltage on the SAPF accuracy. This controlled voltage source injects the compensation voltage needed to mitigate voltage sags and total harmonic distortion into the utility. Fig. 3 introduces a

doi: 10.1049/iet-pel.2012.0570

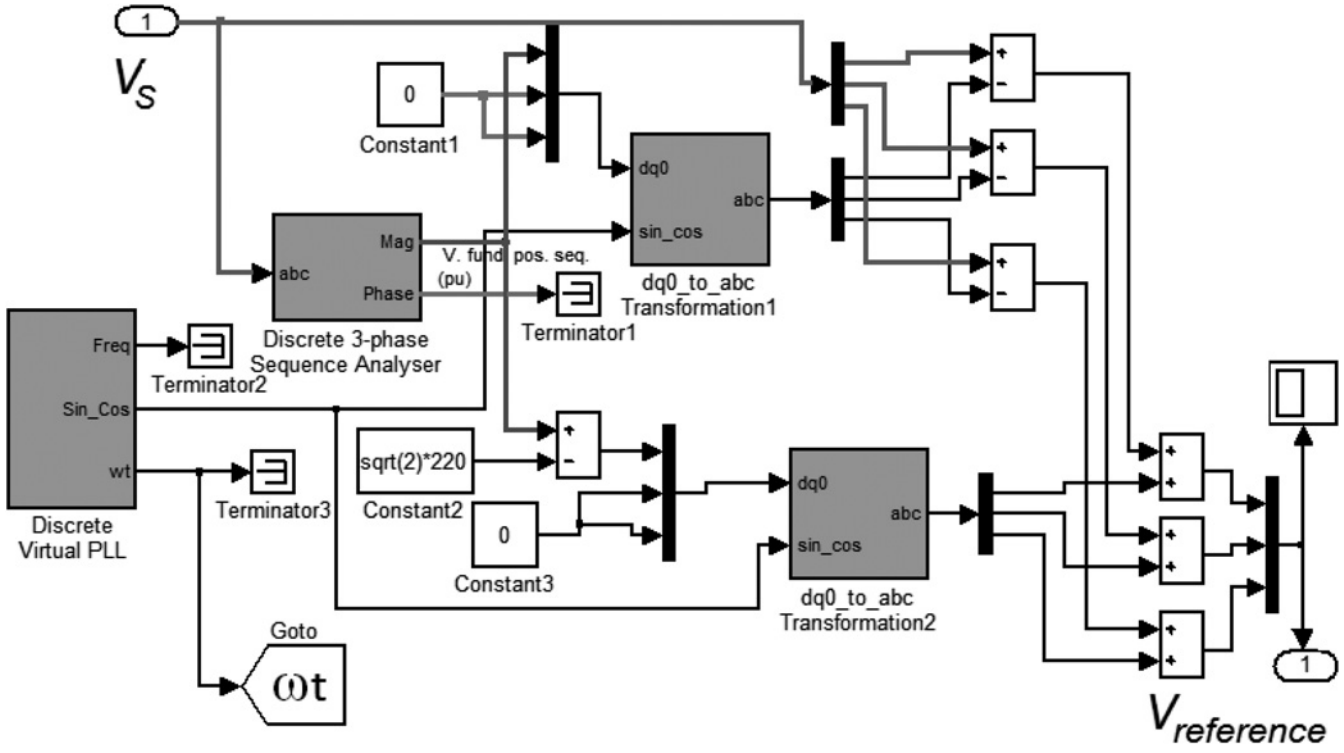

Fig. 3 *Control and modulation of series active filter*

typical SF that is generally used for this aim. As shown in Fig. 3, first the fundamental positive sequence of the source voltages (V_{S1^+}) are obtained. Then, the obtained V_{S1^+} is subtracted from the source voltage, leading to extracting the source voltage oscillations and harmonics. However, the normal source voltage still needs to be tracked just in case of a voltage sag/swell. Second, the controller subtracts the magnitude of the V_{S1}^{+} from its nominal peak $(220\sqrt{2})$, preparing it for the SF to be added to the available references.

This solution leads to the improvement of the SAPF accuracy even in the presence of non-ideal wind turbine voltage waveforms. However, the question is that whether the SF performs as accurate as the SAPF under unbalanced non-linear loads. Owing to the introduced structure of the SF for compensating the source voltage deficiencies, the SF could not be able to force harmonics of the non-linear loads to flow into the SAPF [23]. A current harmonic suppression loop inserted in the control algorithm of the SF (explained later on Fig. 5) in order to simultaneously compensate the source voltage deficiencies, forcing the remained uncompensated current harmonics through the SAPF. Now, the SF highly impedes against frequency components in order to compensate current harmonics drawn because of non-linear diode rectifiers (that show low Z_L in some frequencies) and also the active filter technological limitations as shown in Fig. 4. Considering $G'(j\omega)$ as the SF transfer function and K as the impedance gain when $KG'(j\omega)Z_s(j\omega) + Z_L(j\omega/_{\omega = \omega h})$, then

$$\begin{cases} V_{SF}(j\omega) = KG'(jw)I_S(j\omega), \;\; G'(j\omega) = \begin{cases} 0, \; \omega = \omega_l \\ 1, \; \omega = \omega_h \end{cases} \\ I_S(j\omega) = \dfrac{V_S(j\omega) - V_{VR}(j\omega)}{Z_S(j\omega) + Z_L(j\omega) + KG'(j\omega)} \end{cases} \quad (5)$$

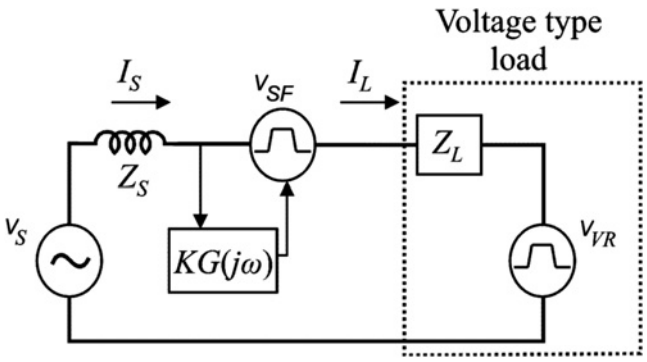

Fig. 4 *SF provides an impedance to affect Z_L of the voltage type capacitive load*

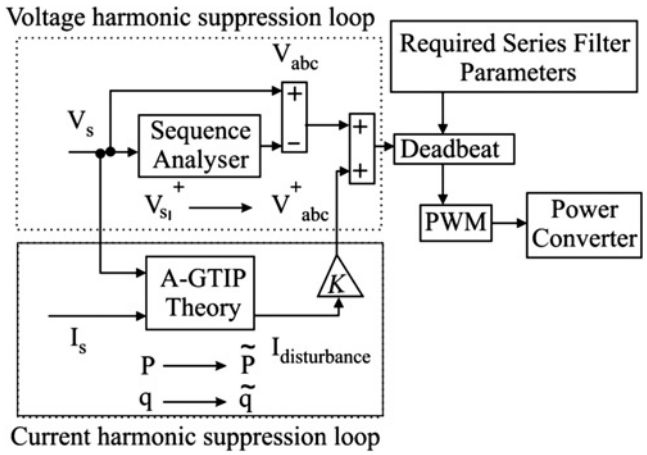

Fig. 5 *Suggested control algorithm for the SF, replacing fundamental current with fundamental voltage*

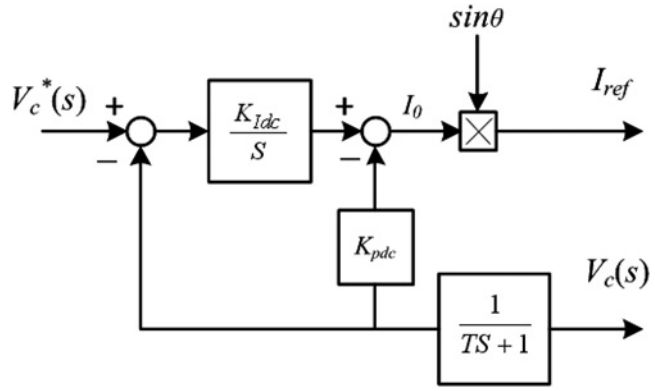

Fig. 6 *Control diagram of the three-phase rectifier suggested in [17]*

It can be shown that the source current tends zero at unwanted frequencies

$$\begin{cases} I_{\mathrm{S}}(\mathrm{j}\omega)\big(\omega=\omega_{\mathrm{h}}\big)=\dfrac{V_{\mathrm{S}}(\mathrm{j}\omega)-V_{VR}(\mathrm{j}\omega)}{Z_{\mathrm{S}}(\mathrm{j}\omega)+Z_{\mathrm{L}}(\mathrm{j}\omega)+KG'(\mathrm{j}\omega)}\simeq 0 \\ V_{\mathrm{SF}}(\mathrm{j}\omega)\big(\omega=\omega_{\mathrm{h}}\big)\simeq Z_{\mathrm{L}}(\mathrm{j}\omega)I_{\mathrm{L}}(\mathrm{j}\omega)+V_{\mathrm{S}}(\mathrm{j}\omega) \end{cases} \quad (6)$$

Fig. 5 introduces an improved control algorithm for series active filter which is suitable for simulation and design purposes. Fundamental component of the source voltage is measured in the harmonic voltage suppression loop to obtain the voltage deficiencies. The source-end current harmonics are obtained in the current harmonic suppression loop by splitting up both the instantaneous oscillating active and non-active power as shown in Fig. 5 using the measured source-end currents (I_{S}). The equivalent source current harmonic ($I_{\mathrm{disturbance}}$) is then multiplied by K to obtain the output voltage of the converter. Further, combination of unified shunt and series active filter produces such references that unwanted frequency components are attenuated according their harmonic order, leading to better currents at the source-end closer to sinusoidal waveforms [see (7) for I_{S}]

$$\begin{cases} I_{\mathrm{L}}(\mathrm{j}\omega)\big(\omega=\omega_h\big)=\dfrac{V_{\mathrm{S}}(\mathrm{j}\omega)-V_{VR}(\mathrm{j}\omega)}{Z_{\mathrm{L}}(j\omega)} \\ I_{\mathrm{S}}(\mathrm{j}\omega)\big(\omega=\omega_h\big)=\dfrac{V_{\mathrm{S}}(\mathrm{j}\omega)-V_{VR}(\mathrm{j}\omega)}{Z_{\mathrm{S}}(\mathrm{j}\omega)+KG'(\mathrm{j}\omega)+\dfrac{Z_{\mathrm{L}}(\mathrm{j}\omega)}{1-G(\mathrm{j}\omega)}}\simeq 0 \\ V_{SF}(\mathrm{j}\omega)\big(\omega=\omega_{\mathrm{h}}\big)\simeq Z_{\mathrm{L}}(\mathrm{j}\omega)I_{\mathrm{L}}(\mathrm{j}\omega)+V_{\mathrm{S}}(\mathrm{j}\omega) \end{cases} \quad (7)$$

Since the combination of the SF and SAPF has a limited power factor correction capability, an independent three-phase converter was suggested in [17] at the source-side to regulate DC-link voltage within the unified compensator by an isolated control circuit as shown in Fig. 6. The independent DC compensator has the advantage of making the shunt activating algorithm simple, lowering the power density of energy storage elements. Although the independent DC-link compensator at the source-side removes the limitation of power factor correction capability, it imposes distortions and harmonics to the source-end currents.

4 Suggesting the AUPQS

The proposed AUPQS also includes a combination of a shunt active filter, a series active filter and an independent AR like that of [17]; however, the AUPQS proposes a 'single-phase' rectifier at the 'load-end' instead of previously raised 'three-phase' rectifier at the 'source-end'. It is shown that the SAPF, activated by the compensation algorithm based on the A-GTIP theory [6], leads to a satisfactory performance under distorted and unbalanced load-terminal voltages in three-phase four-wire systems. Nonetheless, a full harmonic cancellation cannot be achieved because of the technological limitations of the active filters and also under non-linear load conditions. Hence, the suggested improved series active filter (see Fig. 4) is used as a complementary device for the SAPF that is activated by the A-GTIP theory. For example, the developed SF within the proposed AUPQS produces output voltages that can compensate the wind turbine voltage deficiencies. Meanwhile, the remained source-end current harmonics would flow into the shunt part of the AUPQS. Moreover, the independent single-phase AR at the load-end, unlike the previous proposition of a three-phase converter at the source-end, would be able to regulate the DC-link voltage without imposing distortions and harmonics at the source-end. The reason is that the shunt filter of the AUPQS would absorb distortions generated by the independent single-phase AR.

5 Simulations and discussions

To verify the flexibility of the AUPQS, a microgrid was simulated as shown in Figs. 7*a* and *b*. The microgrid consists of a synchronous source (combustion engine/synchronous generator), a wind generator, unbalanced non-linear capacitive load and the compensator (AUPQS). It is supposed that the combustion engine/synchronous generator system is able to supply power to the loads; however, whenever possible, the wind generator is controlled to generate maximum power subjected to saving fuel for the diesel engine. Both the synchronous source and the wind generator contribute to generate the desired maximum power [24]. The simulated wind power plant has a direct driven synchronous generator that includes a variable-speed wind turbine, synchronous generator, two back-to-back power electronic converters as well as one transformer [25–28]. Also, non-linear loads in Fig. 7 consist of three single-phase rectifiers that supply the circuit elements in Fig. 8. The parameters of these loads are introduced in Table 1. Additionally, Fig. 8 demonstrates the details of all the LCL filters in the simulated system.

Other various simulating methods are commonly used for wind turbines such as detailed model, average model and phasor model, based on the range of frequencies involved. The detailed model of the wind turbines is well-suited for observing harmonics over relatively short periods. The presented model includes a 50 kW wind turbine that consists of a synchronous generator connected to a synchronous power system through a rectifier. Both PWM boost converter and PWM DC–AC inverter use IGBT as shown in Fig. 9, where the generated AC voltage and current (and thus power) are converted into DC by using a diode bridge and then inverted back to 50 Hz AC via using the voltage-sourced converter (VSC). This arrangement

doi: 10.1049/iet-pel.2012.0570

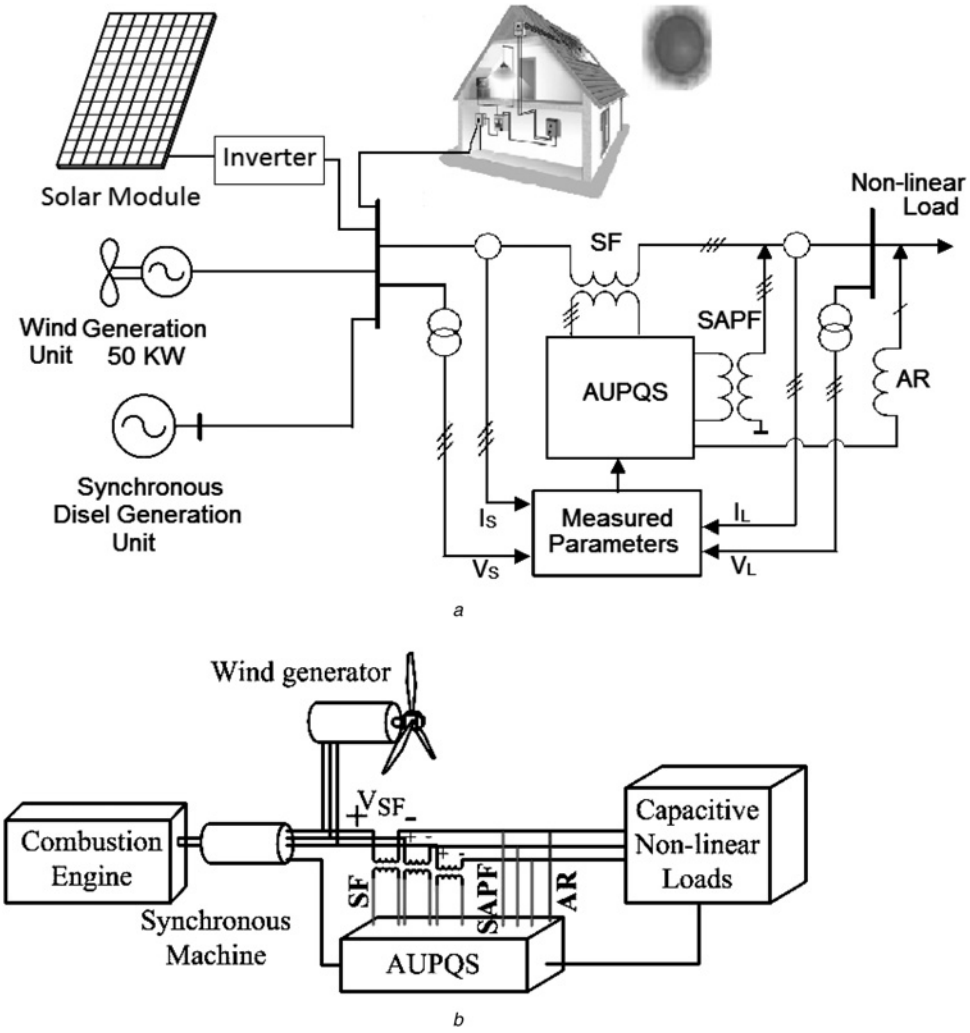

Fig. 7 *Simulated microgrid and AUPQS power circuit*

a Schematic of the using suggested AUPQS in probable microgrid
b Global figure

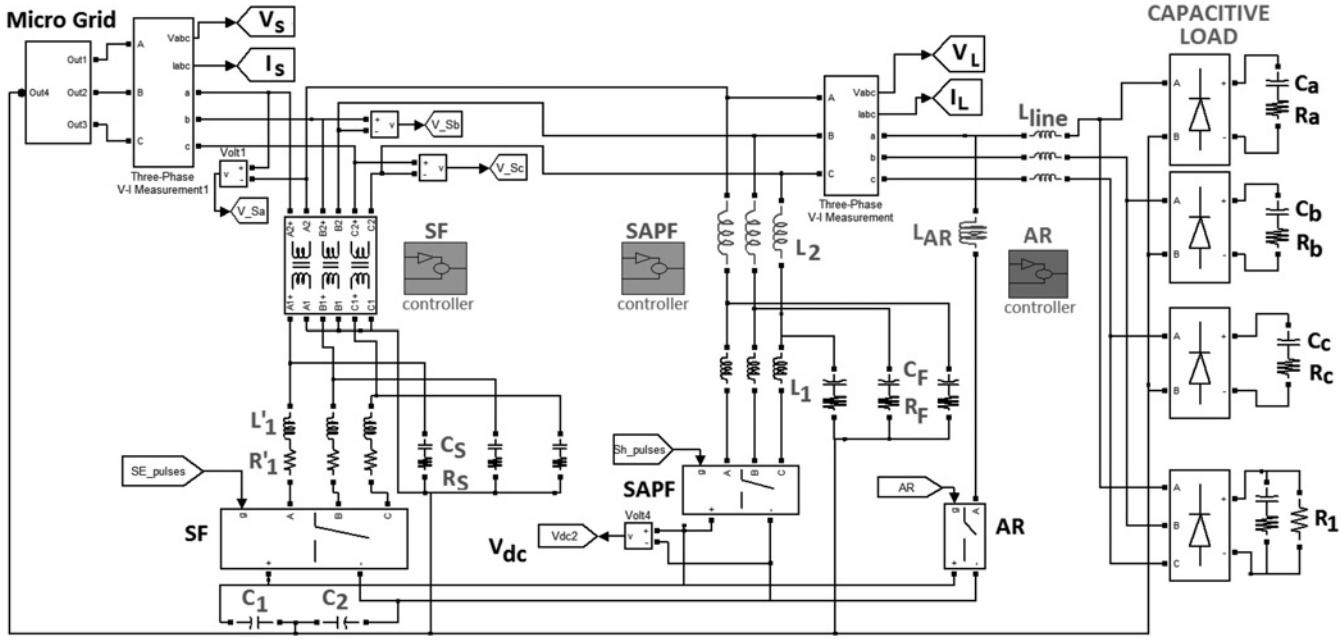

Fig. 8 *Simulated power circuit of the microgrid involving four-wire unbalanced and/or capacitive load*

Table 1 Parameters of single-phase and three-phase loads shown in Fig. 7

R_a	0.5 Ω
C_a	0.5 mF
R_b	0.33 Ω
C_b	50 mF
R_c	0.33 Ω
C_c	5 mF
R_1	3 Ω
R_2	0.5 Ω
C_2	50 mF

Table 2 Parameters of the wind turbine, synchronous generator and boost converter

wind turbine numbers	1
turbine turbine inertia constant (H)	0.432 s
synchronous generator power	50 kVA
synchronous generator voltage (V_{rms})	730 V
generator inertia constant (H)	62 ms
boost converter inductance (L)	1.2 mH
boost converter resistance (R)	5 mΩ
DC bus capacitor	90 mF
nominal DC buse voltage	1100 V
grid-side coupling inductor	0.15 pu
grid-side coupling resistance	0.003 pu

Table 3 Parameters of the AUPQS

AR inductance L_{AR}	1 mH
inductance L_1'	0.6 mH
resistance R_1'	30 mΩ
LCL filter capacitor C_s	220 μF
LCL filter damping resistor R_s	0.5 Ω
SAPF side LCL filter inductance L_1	4.1 mH
grid side LCL filter inductance L_2	0.5 mH
LCL filter capacitor C_f	10 μF
LCL filter damping resistor R_f	20 Ω
SAPF switching frequency	6:9 kHz
SAPF DC-link capacitors (each one)	2 mF
SAPF DC-link voltage	700 V

decouples the wind turbine from the AC system, allowing variable-speed operation of the wind turbine. The VSC is generally controlled to maintain the DC-link capacitor at a constant voltage. This will ensure the power transfer between the DC link and the AC system. In other words, whenever the DC-link voltage falls, the wind turbine active power is not transferred to the AC system, increasing the DC-link voltage instead. The detailed parameters of the wind turbine, synchronous generator and DC–DC boost converter are listed in Table 2. A passive LCL-filter is used to attenuate the unwanted frequency components resulting from the switching modulation of shunt part of the AUPQS

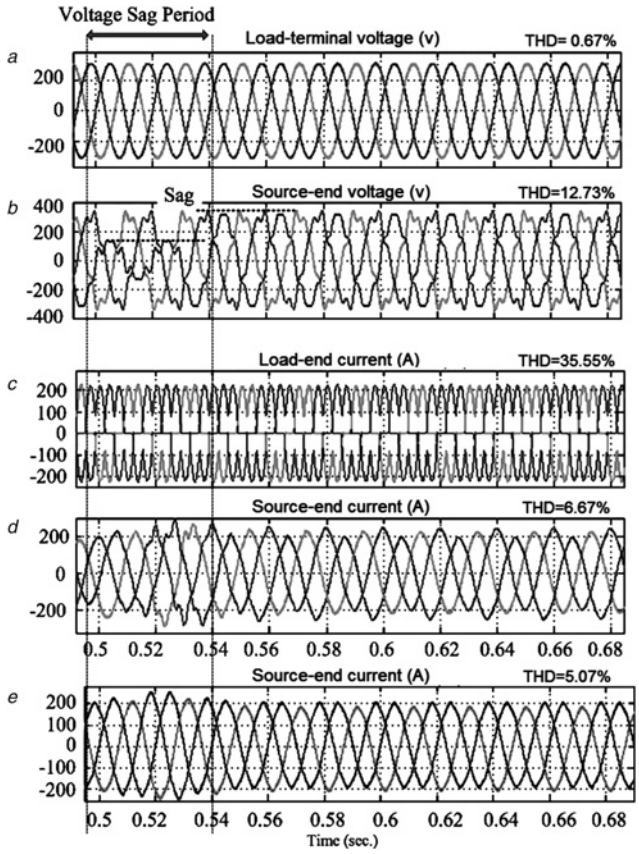

Fig. 10 *Compensation of voltage type capacitive load using both the UPQS and UPQC*

a Three-phase load-terminal voltages (V) (THD = 0.67%) after compensation by the UPQS
b Asymmetrical distorted wind turbine/source voltage (V) (THD 12.73%)
c Three-phase load-end currents (A) (THD = 35.55%)
d Three-phase microgrid/source-end currents (A) after compensation by the UPQS (THD 6.67%)
e Three-phase microgrid/source-end currents (A) after compensation by the UPQC (THD 5.07%)

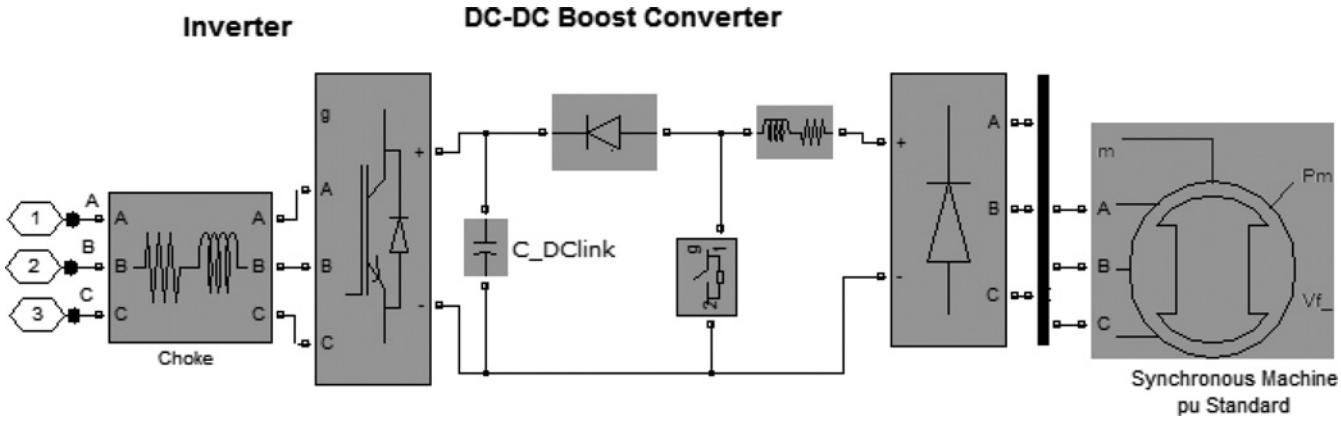

Fig. 9 *Arrangement of the synchronous generator, rectifier, DC–DC boost converter and DC–AC inverter*

doi: 10.1049/iet-pel.2012.0570

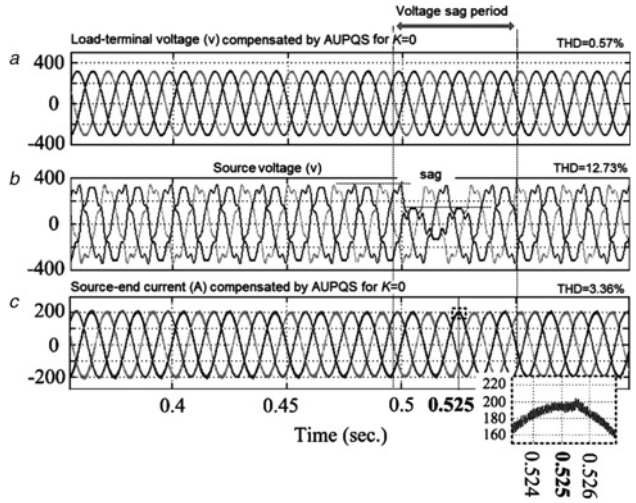

Fig. 11 *Compensation of voltage type capacitive load using the AUPQS for K = 0*

a Three-phase load-terminal voltages (V) (THD = 0.57%) after compensation
b Asymmetrical distorted wind turbine/source voltages (V) (THD 12.73%)
c Three-phase microgrid/source-end currents (A) (THD 3.36%)

[29]. Parameters of the converter and the LCL-filter are listed in Table 3.

Figs. 10*a*–*c* show the compensated load-terminal voltage (i.e. V_L in Fig. 7), microgrid/source voltage (V_S) and load-terminal current (I_L), respectively. It can be seen that the UPQS operates similar to the UPQC (providing a fully compensated harmonic voltages, THD = 0.67%); however, the microgrid/source-end current during the voltage sag condition, as shown in Figs. 10*d* and *e*, still remains non-sinusoidal both for the UPQS and UPQC. This is because of the poor performance of the three-phase DC-link converter of the UPQS at the microgrid-side and the shunt converter of the UPQC used for the DC-link voltage regulation. Moreover, distortions of the source-end currents still could not be suppressed even in three-wire systems. The reason is that the shunt part of both the UPQS and UPQC are controlled based on the *p*–*q* theory that operates correctly only under a balanced system.

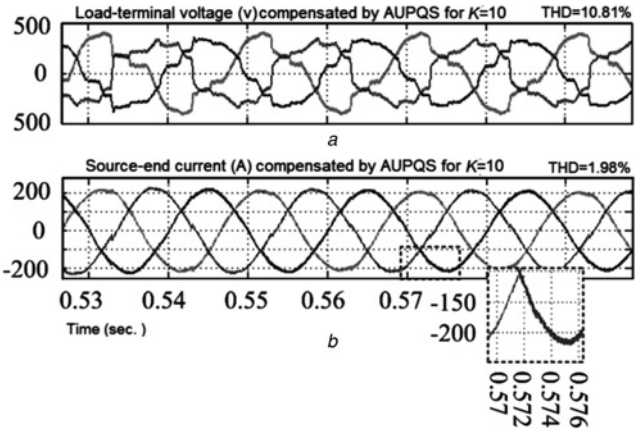

Fig. 12 *Compensation of voltage type capacitive load using the AUPQS for K = 10*

a Three-phase asymmetrical distorted load-terminal voltages (V) (THD = 10.81%) after compensation
b Three-phase microgrid/source-end currents (A) after compensation (THD 1.98%)

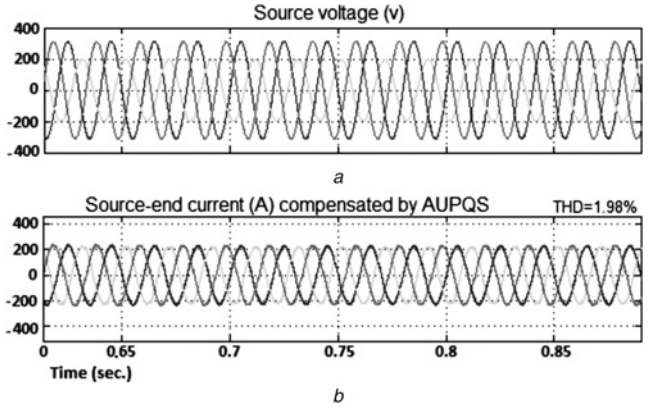

Fig. 13 *THD (in percent) when voltage sag occurs under capacitive load condition*

a Three-phase source voltages
b Source-end currents (THD 1.98%) after compensation

Although the SF of the AUPQS operates toward sinusoidal load-terminal voltages as shown in Fig. 11, without a current suppression loop ($K = 0$), it cannot force the source-end current harmonics to flow into the shunt part of the SAPF (see Fig. 4). Hence, the SAPF, controlled by the A-GTIP theory at the presence of non-linear loads, result in somehow distorted source-end currents above the standard IEEE-519 (THD = 3.36%) as shown in Fig. 11*c*. However, the AUPQS can perfectly compensate voltage sag deficiency as shown in Figs. 11*a* and *b* without any current distortion at the microgrid end because the independent DC-link single-phase AR connected at the load side.

Fig. 12 shows that the proposed the SF of the AUPQS that is equipped with the current suppression loop (for $K = 10$) uplifts the shunt part of the AUPQS accuracy. Therefore the AUPQS under capacitive load conditions would result in purely sinusoidal source-end current. However, the higher the impedance of the current harmonic suppression loop, as shown in Fig. 12*a*, leads to the higher distortions of the load-terminal voltage (THD = 10.81%). Figs. 13*a* and *b* show that the proposed AUPQS would result in purely sinusoidal source-end currents under source voltage sags when the current suppression loop K was set to 10. Figs. 14*a* and *b* summarise the THD of the simulated load-terminal voltages and source-end currents compensated by the AUPQS under different gains K. It can be seen the resultant THD under capacitive load fall within the standard range of the IEEE-519 for $K \geq 10$. Fig. 14*b* presents utilisation of the proposed SF, equipped by the current suppression loop, for the common active filters; it should be noted that for the UPQC, even under balanced three-phase inductive load, the resultant THD is improved by more than 50%. In other words, a full harmonic cancellation can be achieved when the aforementioned uncompensated source-end current harmonics are highly forced to flow into the SAPF. Hence, the resultant THD of the source-end current under balanced inductive load falls below 0.42%.

6 Experimental results

To confirm the validity of the simulations, the SAPF controller of the proposed AUPQS were programmed by MATLAB; then, uploaded on the DSP TMS320F28335. Hence, a test bed was established for emulating the

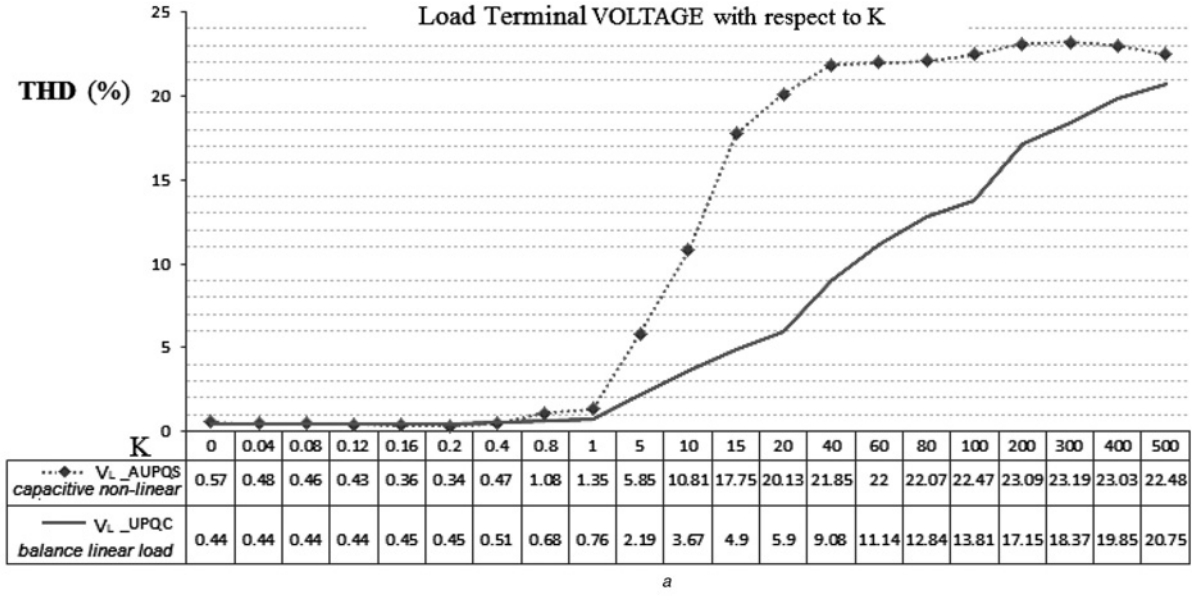

K	0	0.04	0.08	0.12	0.16	0.2	0.4	0.8	1	5	10	15	20	40	60	80	100	200	300	400	500
V_L _AUPQS capacitive non-linear	0.57	0.48	0.46	0.43	0.36	0.34	0.47	1.08	1.35	5.85	10.81	17.75	20.13	21.85	22	22.07	22.47	23.09	23.19	23.03	22.48
V_L _UPQC balance linear load	0.44	0.44	0.44	0.44	0.45	0.45	0.51	0.68	0.76	2.19	3.67	4.9	5.9	9.08	11.14	12.84	13.81	17.15	18.37	19.85	20.75

a

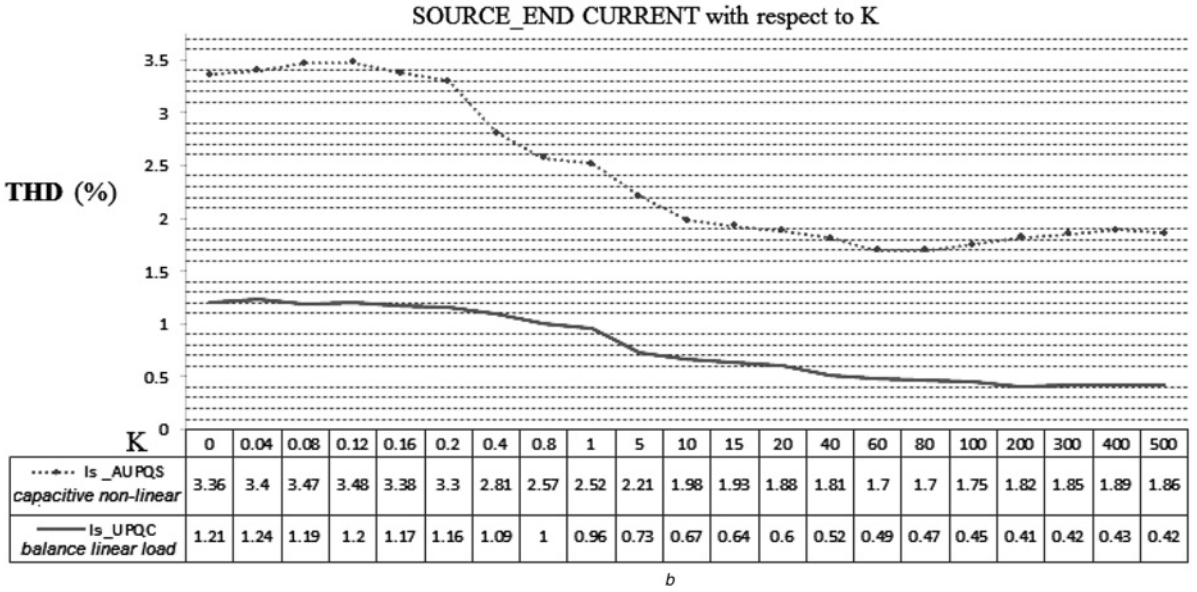

K	0	0.04	0.08	0.12	0.16	0.2	0.4	0.8	1	5	10	15	20	40	60	80	100	200	300	400	500
Is _AUPQS capacitive non-linear	3.36	3.4	3.47	3.48	3.38	3.3	2.81	2.57	2.52	2.21	1.98	1.93	1.88	1.81	1.7	1.7	1.75	1.82	1.85	1.89	1.86
Is_UPQC balance linear load	1.21	1.24	1.19	1.2	1.17	1.16	1.09	1	0.96	0.73	0.67	0.64	0.6	0.52	0.49	0.47	0.45	0.41	0.42	0.43	0.42

b

Fig. 14 *THD (in percent) when the proposed AUPQS is under capacitive loads and a UPQC equipped with the improved SF is under a balanced inductive load*

a Load-terminal voltages
b Microgrid/source-end currents

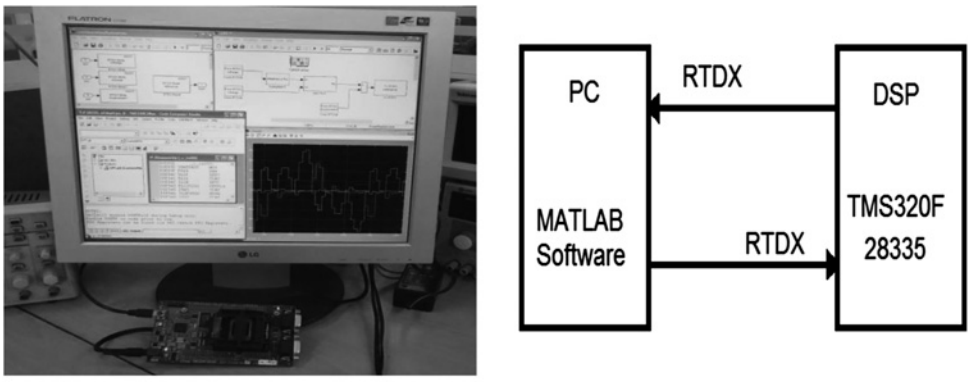

a *b*

Fig. 15 *Relating PC-MATLAB to the DSP*

a Experimental set up
b Schematic diagram

doi: 10.1049/iet-pel.2012.0570

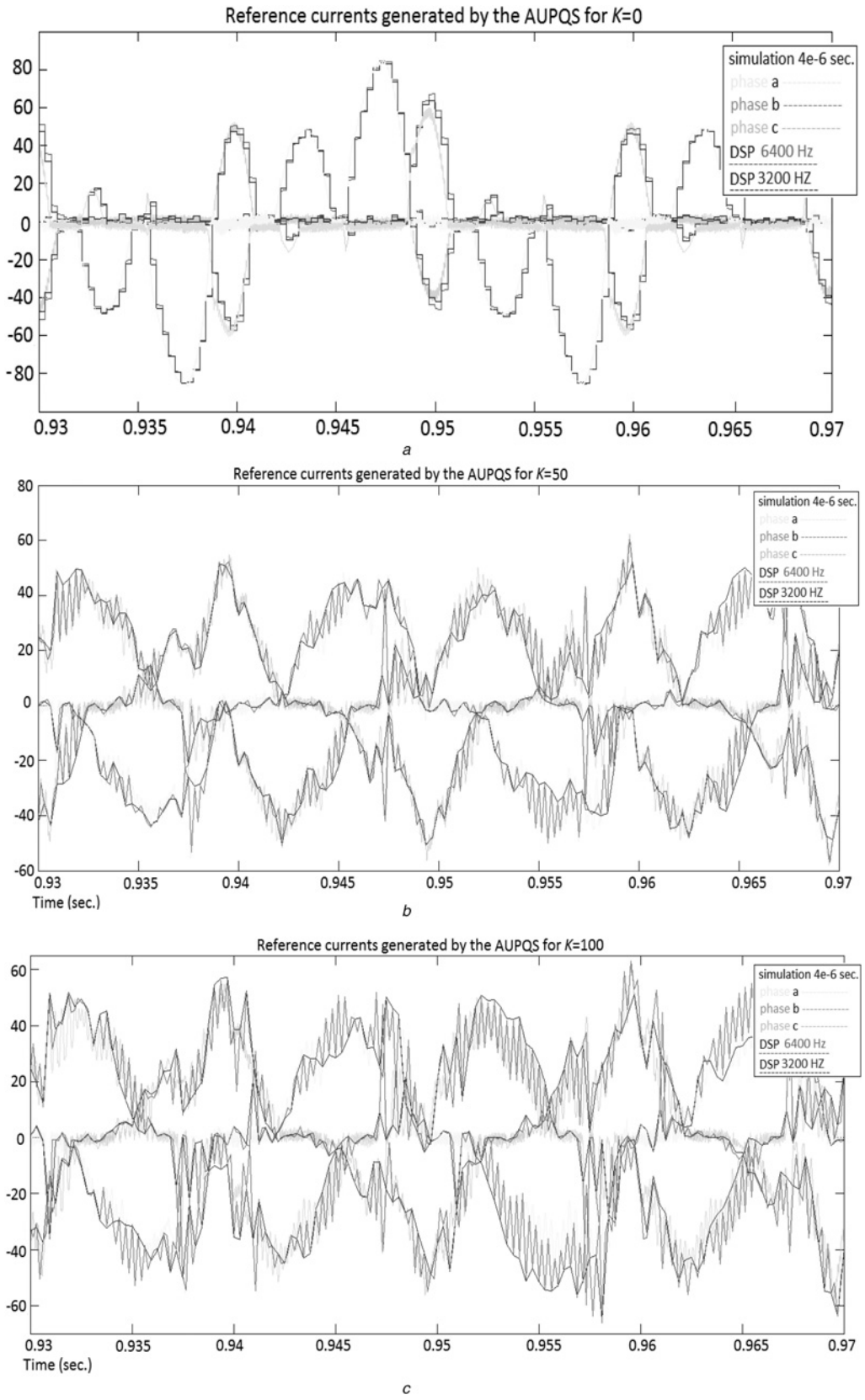

Fig. 16 *Superimposition of experimental and simulation results from the AUPQS reference currents under source voltage harmonics and non-linear load conditions see Table 1 while the sampling time of the DSP are 1/3200 and 1/6400 s, respectively, and the sampling time of the simulations is 4e–6 s*

a $K = 0$
b $K = 50$
c $K = 100$

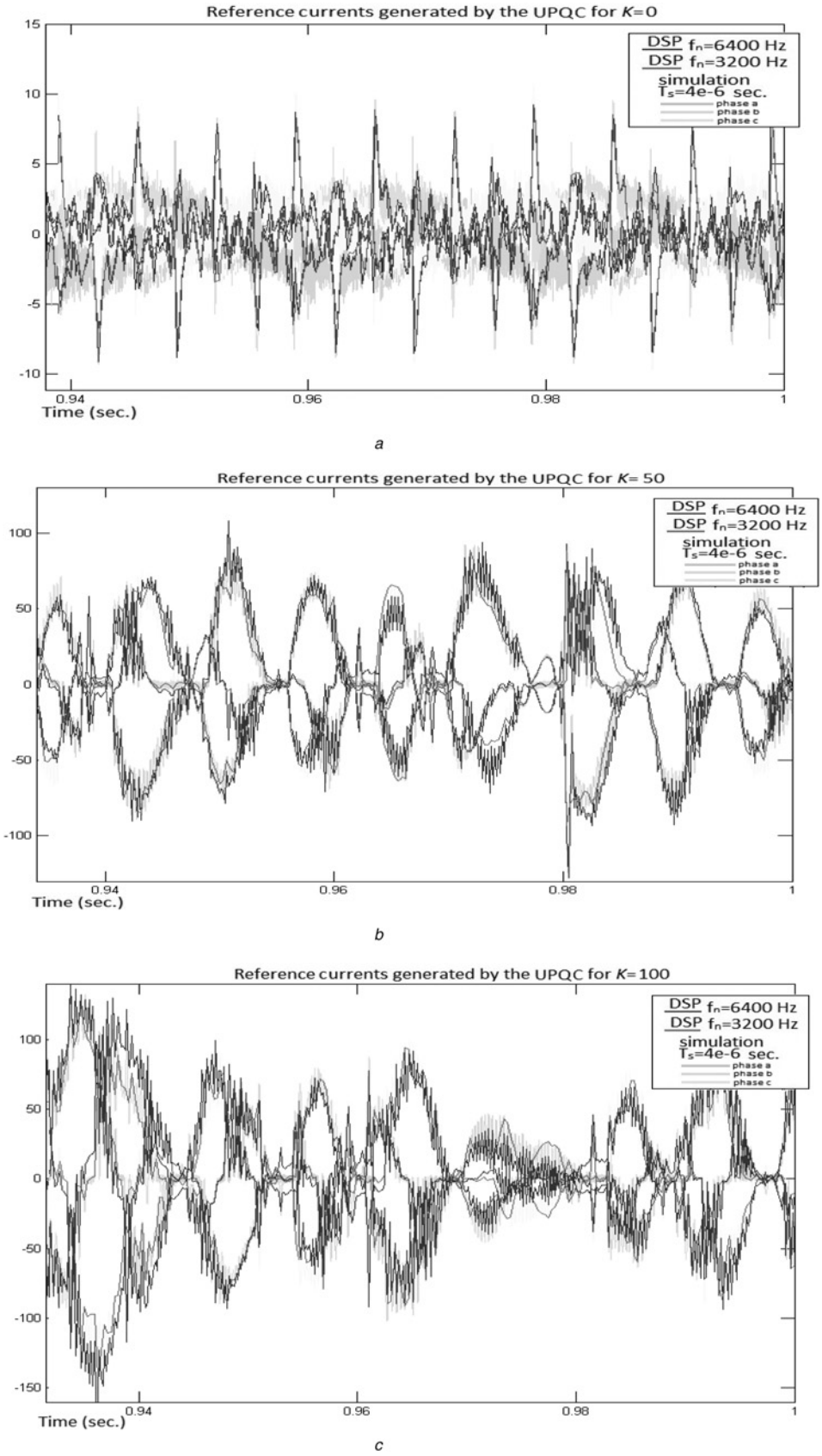

Fig. 17 *Superimposition of experimental and simulation results from the UPQC reference currents under source voltage harmonics and non-linear load conditions (see Table 1) while the sampling time of the DSP are 1/3200 and 1/6400 s, respectively, and the sampling time of the simulation is 4e–6 s*

a $K = 0$
b $K = 50$
c $K = 100$

doi: 10.1049/iet-pel.2012.0570

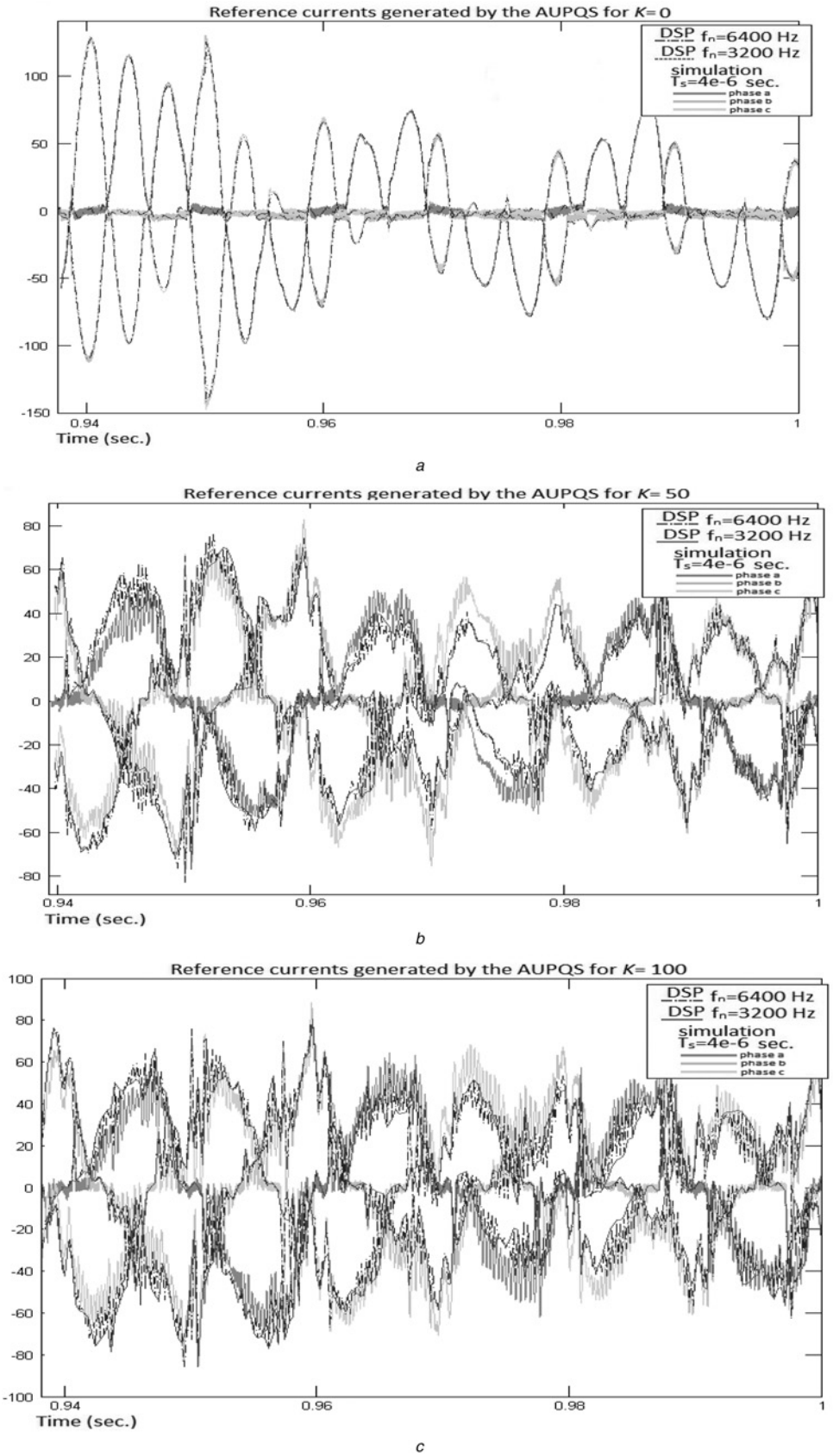

Fig. 18 *Superimposition of experimental and simulation results from the AUPQS reference currents under source voltage sag (0.92–0.95 s) and non-linear load conditions (see Table 1) while the sampling time of the DSP are 1/3200 and 1/6400 s, respectively, and the sampling time of the simulation is 4e–6 s*

a $K = 0$
b $K = 50$
c $K = 100$

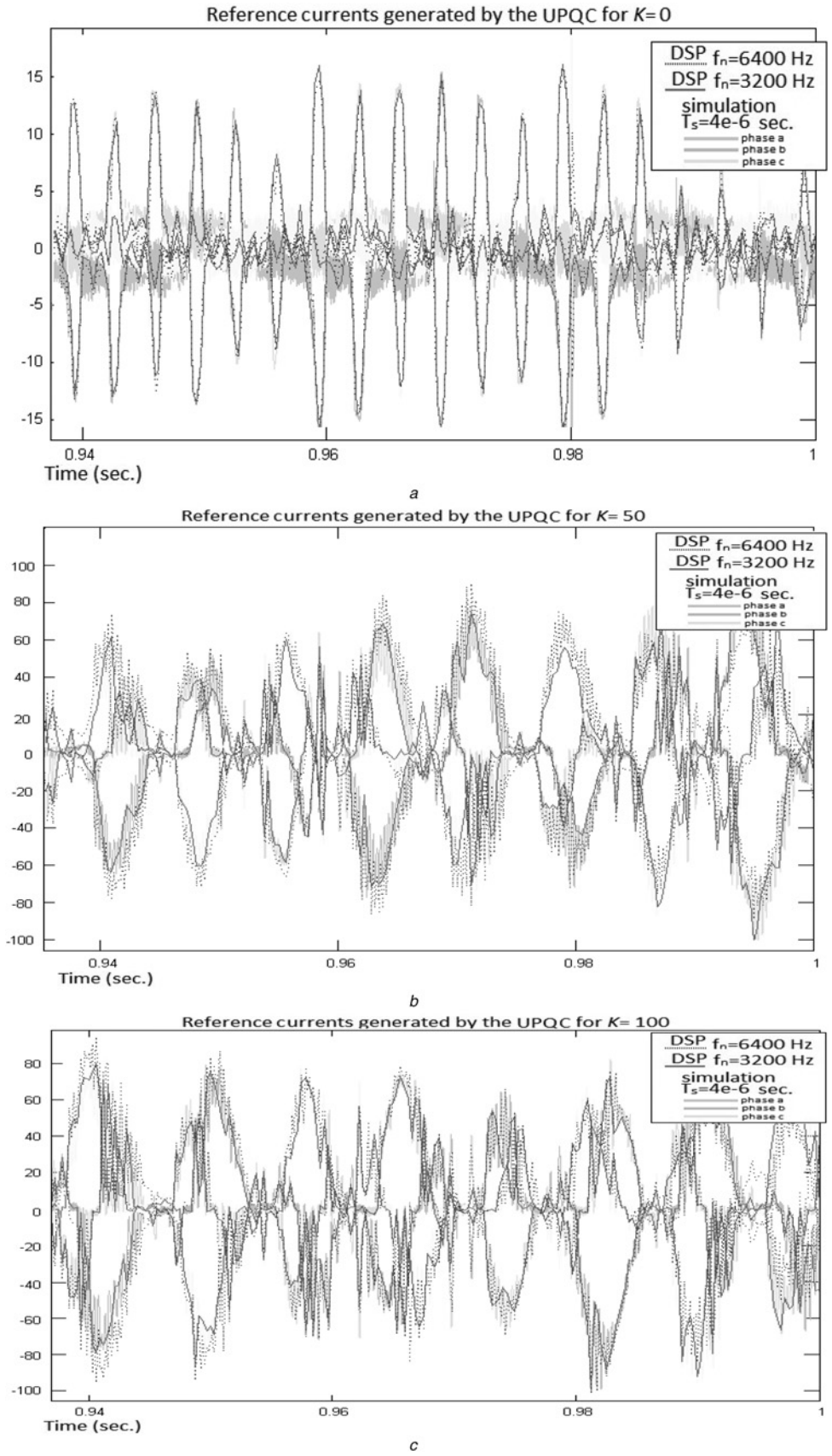

Fig. 19 *Superimposition of experimental and simulation results from the UPQC reference currents under source voltage sag (0.92–0.98 s) and non-linear load conditions (see Table 1 in the appendix) while the sampling time of the DSP are 1/3200 s and 1/6400 s, respectively, and the sampling time of the simulation is 4e–6 s*

a $K = 0$
b $K = 50$
c $K = 100$

doi: 10.1049/iet-pel.2012.0570

proposed tuning technique. Further, samples of active power were taken, and sent to the DSP through the real-time data exchange (RTDX). The data stream is then read through the RTDX with MATLAB in which the USB port of the DSP was used as the RTDX. Fig. 15 shows the stated relationship between the PC and the DSP.

Experimental results show that the reference currents of the SAPF generated by the DSP for different K and under different conditions (see Figs. 16–19) are similar to those of the simulations. Negligible differences between experimental and simulations are because of the sampling frequency of the DSP for the input signals. The higher the sampling frequency, the difference tends to disappear. In general, they are basically the same that proves the validity of the proposed control algorithms. In this section, the discussed simulations (see Section 5 for source voltage harmonics and voltage sag) will separately be analysed in order to show a better and simple look about the generated reference currents by the SAPF. In addition, the parameter K (within the suggested suppression loop of the SF) will obtain different values like 0, 50 and 100. Then, it is analysed how the values of K affect the controller accuracy. The sample rates of the DSP in this study were 3200 and 6400 Hz (Figs. 16–19).

6.1 Source voltage harmonics

The source voltage harmonics can lead to an improper operation of the available active filters as it was discussed in Section 3 [15]. Unlike the available active filters such as UPQC, comparing reference currents (see Figs. 16*a* and 17*a*) demonstrates that the proposed AUPQS can produce highly precise reference currents because of its special physical structure and unique compensation algorithm. In other words, the AUPQS can recognise and suppress a large variety of the source-end current harmonics. Figs. 16*a–c* also show that increasing the value of K within the suggested suppression loop leads the AUPQS to generate much more accurate reference currents. Therefore a higher level of sinusoidal source-end currents would be possible [see (7) alongside Fig. 14 for I_S]. Figs. 17*a–c* demonstrate that when even the proposed suppression loop is added to such available active filters as the UPQC (see Figs. 14*a* and *b*), the SF can effectively force the remaining source-end current harmonics to pass through the SAPF.

6.2 Voltage sag

Fig. 18*a* shows how the shunt filter of the AUPQS under voltage sag generates the needed reference currents to absorb distortions produced by the suggested AR. The suggested single-phase AR at the load-side regulates the DC-link voltage, acting as a single-phase load while supplies the active power needed for the SF. On the contrary, the available active filters cannot produce accurate reference currents under voltage sag condition as it can be seen in Fig. 19*a*. The reason is that the SAPF of the UPQC simultaneously suppress the source-end current harmonics, whereas regulates the DC-link voltage, imposing distortions and harmonics at the source-end (see Figs. 10*d* and *e*). Nonetheless, the proposed single-phase rectifier of the AUPQS at the load-side works as a single-phase load, leading to less distorted and much precise reference currents as showed in Figs. 16 and 18*a–c*. Figs. 18*a–c* and 19*a–c* also show that under non-linear load conditions the higher the value of K in the suppression loop of the SF, the more accurate the reference currents of the SAPF, and the less the source-end current harmonics.

7 Conclusion

This paper analyses the validity of available solutions for eliminating the consequences of distorted and unbalanced voltage waveforms on the SAPF accuracy that is generated because of the wind turbine operation. Mathematical analysis reveals that available compensating algorithms suffer from unbalance, distortion and zero sequence components because of the presence of non-linear loads. Considering the new compensation algorithm based on the A-GTIP theory, here it is proposed the AUPQS for three-phase four-wire systems. Moreover, by improving the SF algorithm of the AUPQS, the non-linear capacitive load type harmonics as well as the remained current harmonics because of the technological limitations of the active filters can be attenuated considerably, forcing them to be supplied by the shunt filter of the AUPQS. Meanwhile, by designing an independent single-phase AR at the load side, the proposed AUPQS would be able to regulate the DC-link voltage without any distortion caused by the regulating converter. Hence, a full cancellation of the source-end zero sequence current as well as harmonic suppression can be achieved in three-phase four-wire systems. Therefore purely sinusoidal wind turbine-end currents lead to high electrical efficiency for the power system. Effectiveness of the proposed AUPQS is verified by simulations.

8 References

1 Sabin, D., Sundaram, A.: 'Quality enhances reliability', *IEEE Spectr.*, 1996, **33**, (2), pp. 34–41
2 Fryze, S.: 'Effective wattless and apparent power in electrical circuits for the case of non-sinusoidal waveform of current and voltage'. Elektrotechnische zeitschr, 1932, pp. 596–599
3 Czarnecki, L.S.: 'Minimization of unbalanced and reactive currents in three-phase asymmetrical circuits with non-sinusoidal voltage', *IEE Proc. B*, 1992, **139**, (4), pp. 347–354
4 Peng, F.Z., Lai, J.S.: 'Generalized instantaneous reactive power theory for three-phase power systems', IEEE 00189456. 1996
5 Tavakoli Bina, M.: 'Inactive power harmonics control', 2003, pp. 46–50
6 Pashajavid, E., Tavakoli Bina, M.: 'Zero-sequence component and harmonic compensation in four-wire systems under non-ideal waveforms', Przegląd Elektrotechniczny (Electrical Review), R. 85 NR 10/2009
7 Depenbrock, M.: 'The FBD-method, a generally applicable tool for analyzing power relations', *IEEE Trans. Power Syst.*, 1993, **8**, (2), pp. 381–387
8 Czarnecki, L.S.: 'Currents' physical components (CPC) in circuits with non-sinusoidal voltages and currents part 2: three-phase three-wire linear circuits', *J. Electr. Power Qual. Utilization*, 2005, **XI**, (2), pp. 3–14
9 Tenti, P., Tedeschi, E., Mattavelli, P.: 'Cooperative operation of active power filters by instantaneous complex power control'. Proc. Seventh Int. Conf. Power Electronics and Drive Systems, November 2007
10 Kim, H.S., Akagi, H.: 'The instantaneous power theory on the rotating 694 *p–q–r* reference frames'. Proc. IEEE/PEDS Conf., Hong Kong, July 1999, pp. 422–427
11 Depenbrock, M., Staudt, V., Wrede, H.: 'Concerning instantaneous power compensation in three-phase systems by using *p–q–r* theory', *IEEE Trans. Power Electron.*, 2004, **19**, (4), pp. 1151–1152
12 Aredes, M., Akagi, H., Watanabe, E.H., Salgado, E.V., Encarnação, L. F.: 'Comparisons between the *p–q* and *p–q–r* theories in three-phase four-wire systems'. IEEE Trans. Power Electron., paper accepted in October 2008
13 Oliveira, F., Madureira, A., Donsión, M.P.: 'Experimental study of power quality in wind farms'. ICREPQ'04, 2004
14 Madureira, A., Oliveira, F., Donsión, M.P.: 'Statistical study of power quality in wind farms'. ICREPQ'04, 2004

15 Rahmani, B., Tavakoli Bina, M.: 'Eliminating the consequence of non-ideal waveforms on the SAPF accuracy due to the wind turbine operation within a micro-grid'. EWEA Conf., April 2011
16 Watanabe, E.H., Aredes, M., Akagi, H.: 'The *p–q* theory for active filter control: some problems and solutions'. Revista Controle Automação, 2004, **15**, (1), pp. 78–84
17 Graovac, D., Katic, V.A., Rufer, A.: 'Power quality problems compensation with universal power quality conditioning system', *IEEE Trans. Power Deliv.*, 2007, **22**, (2), pp. 968–970
18 Suvire, G.O.: 'Mitigation of problems produced by wind generators in weak systems'. PhD thesis, San Juan National University, Argentina, ly, (in Spanish)
19 Goya, T., *et al.*: 'Torsional torque suppression of decentralized generators based on h∞ control theory'. Int. Conf. Power System Transient (IPST'2009), Kyoto, 2–6 June 2009
20 Rahmani, B., Tavakoli Bina, M.: 'The compensation algorithm based on advanced GTIP theory for switching compensators and possibility of the micro-grids' stability'. PSC 25th Int. Power System Conf., 10-F-PQA-1205, 2010, (in Farsi)
21 Cheng, D.K.W., Lee, Y.S.: 'Harmonic compensation for nonlinear loads by active power'. Power Electron. Drive Syst., (PEDS'99c), 1999
22 Hussien, Z.F., Atan, N., Abidin, I.Z.: 'Shunt active power filter for harmonic compensation of nonlinear loads'. Power Engineering Conf., (PECON 2003), 2003
23 Fujita, H., Akagi, H.: 'The unified power quality conditioner: the integration of series and shunt-active filters', *IEEE Trans. Power Electron.*, 1998, **13**, (2), pp. 315–322
24 Monteiro, L.F.C., Afonso, J.L., Pinto, J.G., Watanabe, E.H., Aredes, M., Akagi, H.: ' Compensation algorithms based on the *p–q* and CPC theories for switching compensators in micro-grids'. IEEE 978-1-4244-3370, 2009
25 Petrovic, V., Jelavic, M., Peric, N.: 'Identification of wind turbine model for individual pitch controller design'. Proc. 43rd Int. Universities Power Engineering Conf. (UPEC'08), September 2008, pp. 1–5
26 Slootweg, J.G., Polinder, H., Kling, W.L.: 'Initialization of wind turbine models in power system dynamics simulations'. Power Tech. Proc., 2001 IEEE Porto, vol. 4, September 2001
27 Yildirim, D., Gurkaynak, Y.: 'An algebraic method for maximum power point tracking in wind turbines'. Proc. Second Int. Power and Energy Conf. (PECon 2008), 1–3 December 2008, pp. 445–450
28 Yiguang, C., Zhiqiang, W., Yonghuan, S, Lingbing, K.: 'A control strategy of direct driven permanent magnet synchronous generator for maximum power point tracking in wind turbine application'. Int. Conf. Electrical Machines and Systems (ICEMS 2008), 17–20 October 2008, pp. 3921–3926
29 Tavakoli Bina, M., Pashajavid, E.: 'An efficient procedure to design passive LCL-filters for active power filters', *Electr. Power Syst. Res.*, 2009, **79**, (4), pp. 606–614

doi: 10.1049/iet-pel.2012.0570